Electronic Supplementary Information: Phage probes couple to DNA relaxation dynamics to reveal universal behavior across scales and regimes

Farshad Safi Samghabadi,[1] Juexin Marfai,[2] Camyla Cueva,[2] Mehdi Aporvari,[2] Philip Neill,[2] Maede Chabi,[3] Rae M. Robertson-Anderson,[2] and Jacinta C. Conrad[1]

[1] *Department of Chemical & Biomolecular Engineering, University of Houston, Houston, TX 77204*

[2] *Department of Physics and Biophysics, University of San Diego, San Diego, CA 92110*

[3] *Department of Biomedical Engineering, University of Houston, Houston, TX 77204*

I. HYDRODYNAMIC RADIUS OF PHAGE

We measured the hydrodynamic radius of the phage in electrolyte solutions as $R_{\mathrm{h,M13}} \approx 107$ nm [1]. The estimated $R_{\mathrm{g,p}} \approx 161$ nm of the M13 in electrolyte solutions is much smaller than that of a rigid rod of corresponding length $R_{\mathrm{g,rigid}} \approx 260$ nm, suggesting that the M13 phage is semiflexible.

II. ROD DIFFUSION MODEL

The Broersma model predicts the diffusivity of high aspect ratio rigid nanorods (often for aspect ratios greater than 3.5) [2, 3]. According to this model, the translational diffusion coefficient of a rod with the length of L and diameter of d diffusing in a homogeneous medium with viscosity η at temperature T is given by $D_{\mathrm{Br,T}} = (k_{\mathrm{B}}T/3\pi\eta L)[\delta - 1/2(\gamma_{\parallel} + \gamma_{\perp})]$, where

$$\delta = \ln(2L/d) \tag{1}$$

$$\gamma_{\parallel} = 0.807 + 0.15/\delta + 13.5/\delta^2 - 37/\delta^3 + 22/\delta^4 \tag{2}$$

$$\gamma_{\perp} = -0.193 + 0.15/\delta + 8.1/\delta^2 - 18/\delta^3 + 9/\delta^4 \tag{3}$$

III. PHAGE DATA DO NOT COLLAPSE WITH IONIC-STRENGTH-DEPENDENT c^*

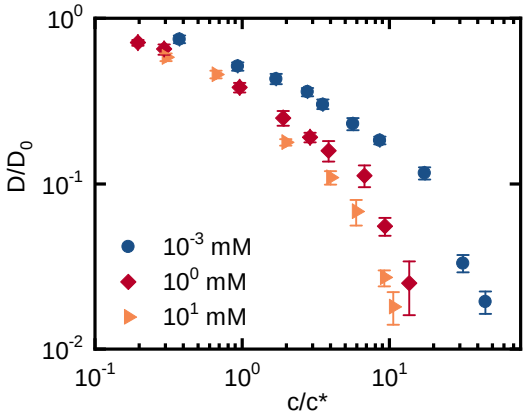

FIG. S1. Phage diffusivity D, normalized by the corresponding tracer value D_0, as a function of normalized concentration c/c^* of 5.9 kbp DNA for NaCl concentrations of 10^{-3} (blue circles), 10^0 (red diamonds), and 10^1 (orange right-pointing triangles) mM.

IV. BULK RHEOLOGY

A Discovery Hybrid Rheometer (DHR-3, TA Instruments) equipped with a 40 mm stainless steel parallel plate upper geometry and Peltier temperature-controlled bottom geometry was used to measure the bulk rheology of the 5.9 kbp DNA solutions at 22°C. 180 μL of the DNA sample was gently loaded onto the bottom plate to ensure bubble-free solutions. The upper geometry was then lowered until the gap was filled (~90 – 120 μL). The geometry was sealed with mineral oil to avoid solution evaporation. To determine the linear viscoelasticity regime, amplitude strain sweep measurements were carried out at angular frequencies ω = 1, 10, and 100 rad s^{-1}. These measurements showed that the linear regime extended up to strains $\gamma = 10\%$, so a strain of $\gamma = 5\%$ was chosen to perform frequency sweeps to ensure linear regime behavior. The frequency-dependent storage modulus $G'(\omega)$ and loss modulus $G''(\omega)$ was measured for ω = 0.001 – 600 rad s^{-1}. Data points with a generated torque below 0.01 μN·m and/or a raw phase angle above 175° were removed to meet the instrument sensitivity limit and to avoid inertial effects, respectively. The instrument was calibrated

for inertia and torque before each measurement.

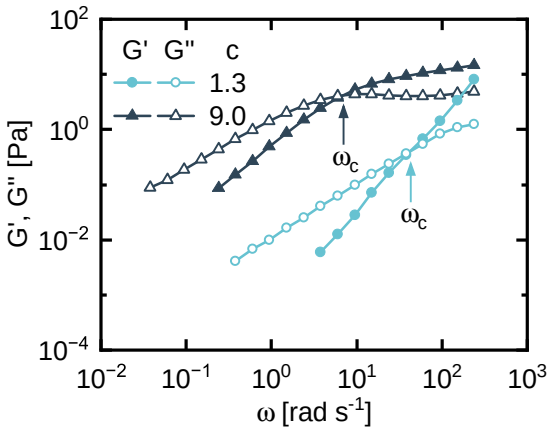

FIG. S2. Linear frequency-dependent storage modulus $G'(\omega)$ (filled symbols) and loss modulus $G''(\omega)$ (open symbols) as a function of angular frequency ω for solutions of 5.9 kbp DNA solutions at ionic strength $I = 10^{-3}$ mM and DNA concentrations of $c = 1.3$ mg mL^{-1} $\simeq 5c^*$ (cyan) and $c = 9.0$ mg mL^{-1} $\simeq 34c^*$ (dark blue). Arrows indicate the frequency at which G' becomes larger than G'', a measure of the longest relaxation time of the system $\tau = 2\pi\omega_c^{-1}$.

V. SUPPLEMENTARY MSD PLOTS

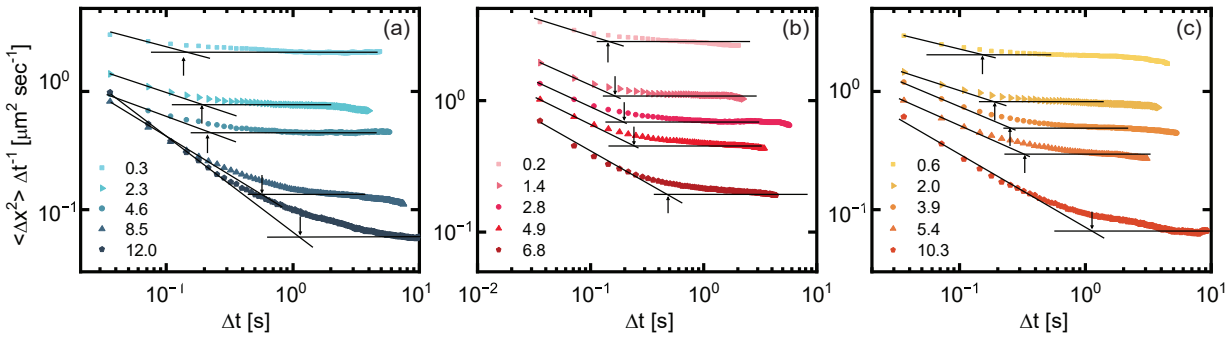

FIG. S3. Normalized mean-squared displacement $\langle \Delta x^2 \rangle \Delta t^{-1}$ as a function of lag time Δt for M13 phage for solutions with varying concentration of 5.9 kbp DNA and ionic strengths of (a) 10^{-3}, (b) 10^{0}, and (c) 10^{1} mM NaCl. Solid lines represent the tangent lines. The concentration units are in mg mL^{-1}. Arrows indicate the intersection of the tangent lines which corresponds to the crossover time from the subdiffusive to diffusive regime.

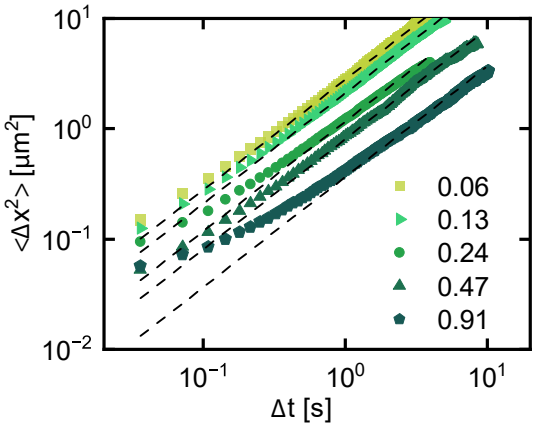

FIG. S4. Mean-squared displacement $\langle \Delta x^2 \rangle$ as a function of lag time Δt for M13 phage for solutions with varying concentration of 115 kbp DNA and ionic strength of 10^{-3} mM NaCl. The concentration units are mg mL^{-1}. Dashed lines represent linear scaling $\langle \Delta x^2 \rangle \sim \Delta t$ indicative of normal diffusion.

VI. UNIVERSAL DIFFUSIVITY COLLAPSE FOR ALL DNA MOLECULAR WEIGHTS

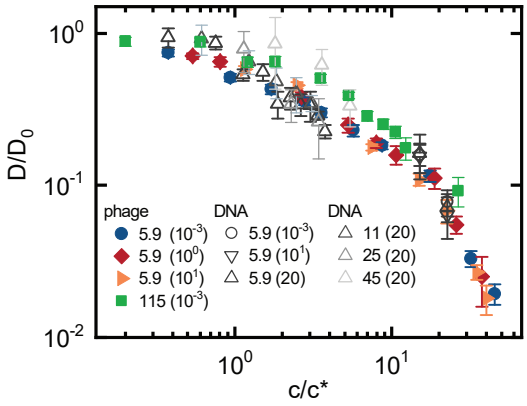

FIG. S5. Normalized diffusion coefficients D/D_0 for phage probes and DNA as a function of concentration c scaled by the overlap concentration c^*. The closed symbols are the phage diffusion coefficients in solutions of: 5.9 kbp DNA at ionic strength I (mM) of 10^{-3} (blue circles), 10^0 (red diamonds), and 10^1 (orange right-pointing triangles); 115 kbp DNA at $I = 10^{-3}$ (green closed squares). The open symbols are diffusion coefficients for DNA molecules of: 5.9 kbp DNA at $I = 10^{-3}$ mM (deep grey circles), $I \simeq 10^1$ mM (TE buffer) (deep grey down-pointing triangles), and $I \simeq 20$ mM (TE with 10 mM NaCl) (deep grey up-pointing triangles); 11 kbp (dark grey triangles), 25 kbp (grey triangles), and 45 (light grey triangles) at $I \simeq 20$ mM (TE with 10 mM NaCl). The open symbols data are reproduced from Ref. [4] (semidilute) or measured in this study (entangled).

VII. ERGODICITY BREAKING PARAMETER

We calculated the ergodicity-breaking (EB) parameter EB = $\left[\left\langle(\delta x^2)^2\right\rangle - \langle\Delta x^2\rangle^2\right]/\langle\Delta x^2\rangle^2$, where δx^2 is the time-averaged squared displacement of each trajectory.

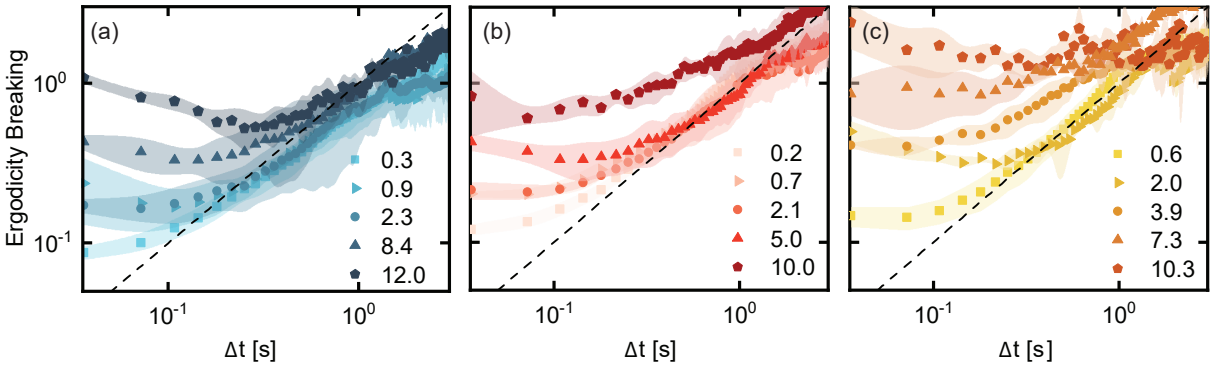

FIG. S6. Ergodicity breaking (EB) parameter as a function of lag time Δt for M13 phage for solutions with various concentrations of 5.9 kbp DNA and ionic strengths of (a) 10^{-3}, (b) 10^{0}, and (c) 10^{1} mM. The concentration units are mg mL^{-1}. Dashed lines indicate the Brownian motion asymptote [5]. The shaded region represents the standard deviation of four measurements per sample.

VIII. PROBABILITY DISTRIBUTION OF DISPLACEMENTS (PDD)

The self-part of the van Hove correlation function $G_s(\Delta x, \Delta t) = \frac{1}{N}\left\langle \sum_{i=1}^{N} \delta((x_i(t) - x_i(t + \Delta t) - \Delta x)\right\rangle$, where δ is the Dirac delta function and N is the number of trajectories, was used to characterize the probability distribution of displacements.

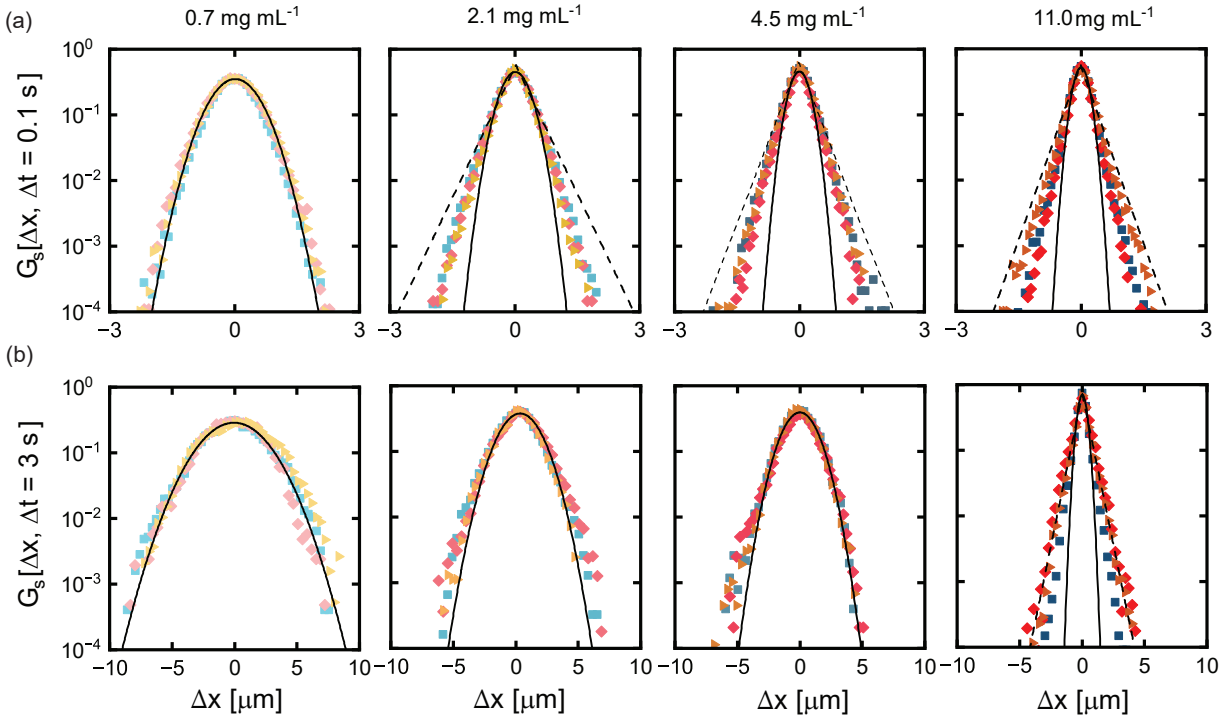

FIG. S7. Probability distribution of displacements $G_s(\Delta x, \Delta t)$ as a function of displacement Δx (μm) for M13 phage in solutions of 5.9 kbp DNA with various DNA concentrations and ionic strength of 10^{-3} (■), 10^{0} (◆), and 10^{1} (▶) mM NaCl at lag time (a) $\Delta t = 0.1$ and (b) $\Delta t = 3$ s. The solid and dashed curves indicate the Gaussian and a sum of a single Gaussian and single exponential prediction, respectively.

IX. PRINCIPAL COMPONENT ANALYSIS (PCA)

To evaluate the directional asymmetry in the motion of spherical and phage particles, we performed Principal Component Analysis (PCA) on the particle trajectories and analyzed the van Hove distributions along the major and minor axes. PCA is a statistical method that decomposes the covariance matrix of particle displacements to identify the dominant

directions of motion. For each trajectory, we first subtracted the mean value from the displacements in both directions, $x_{\text{centered}} = x - \langle x \rangle$ and $y_{\text{centered}} = y - \langle y \rangle$ to center the motion. The centered coordinates were then normalized by dividing by their respective standard deviations, $x_{\text{normalized}} = x_{\text{centered}}/\sigma_x$ and $y_{\text{normalized}} = y_{\text{centered}}/\sigma_y$, to eliminate the effect of various trajectory scales. PCA was applied to the normalized trajectory data to calculate the covariance matrix from which the eigenvalues, λ_1 (major axis) and λ_2 (minor axis), were extracted. The eigenvalue ratio, λ_1/λ_2, was then calculated for each trajectory and a histogram of the eigenvalue ratios was generated across all trajectories as shown in Figure S8.

For solutions of 0.7 mg mL^{-1} (semidilute) and 2.9 mg mL^{-1} (entangled), the van Hove distributions along the major and minor axes show no significant differences for both spherical and phage particles. Similarly, the probability of eigenvalue ratios peaked close to 1, indicating that motion is mainly isotropic with no significant directional differences in displacement magnitudes. This analysis supports the assumption that averaging displacements across all directions is a valid approach for calculating the mean squared displacements (MSDs) and reinforces the robustness of the center-of-mass diffusion analysis for phage across various concentration regimes.

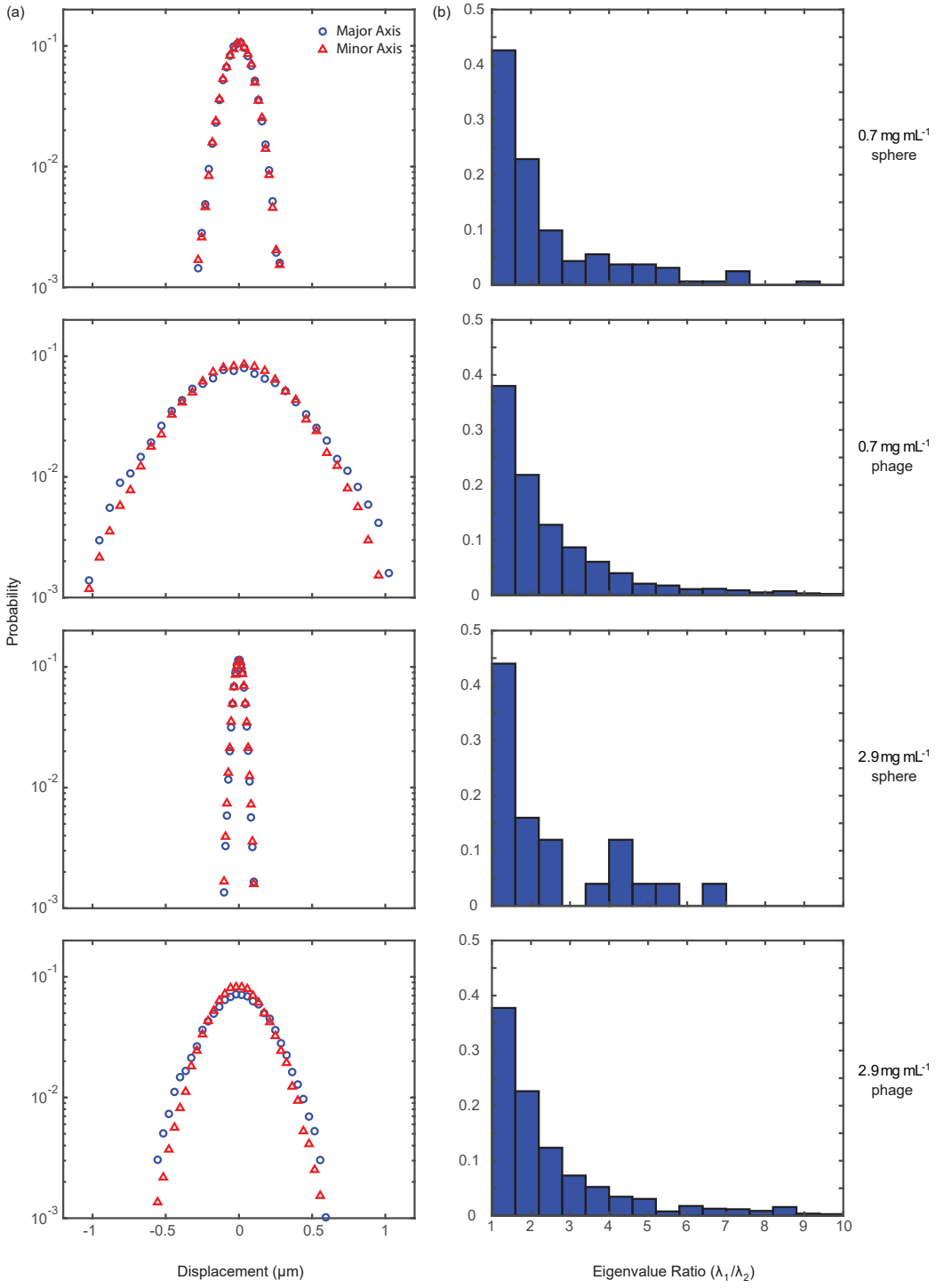

FIG. S8. Column (a) probability distribution of displacements along the major and minor axes as a function of displacement at lag time $\Delta t = 0.036$ s and column (b) probability distribution of eigenvalue ratio λ_1/λ_2 for 1 μm spheres and M13 phage in solutions of 5.9 kbp DNA with DNA concentrations of 0.7 (semidilute) and 2.9 mg mL^{-1} (entangled) and ionic strength of 10^0 mM NaCl.

REFERENCES

[1] F. Safi Samghabadi, A. H. Slim, M. W. Smith, M. Chabi, and J. C. Conrad, Dynamics of filamentous viruses in polyelectrolyte solutions, Macromolecules **55**, 10694 (2022).

[2] S. Broersma, Viscous force constant for a closed cylinder, J. Chem. Phys. **32**, 1632 (1960).

[3] S. Broersma, Viscous force and torque constants for a cylinder, J. Chem. Phys. **74**, 6989 (1981).

[4] R. M. Robertson and D. E. Smith, Self-diffusion of entangled linear and circular DNA molecules: Dependence on length and concentration, Macromolecules **40**, 3373 (2007).

[5] R. Metzler, J.-H. Jeon, A. G. Cherstvy, and E. Barkai, Anomalous diffusion models and their properties: non-stationarity, non-ergodicity, and ageing at the centenary of single particle tracking, Phys. Chem. Chem. Phys. **16**, 24128 (2014).